Austrian Journal of Earth Sciences | Volume 107/2 | 23 - 36 | Vienna | 2014

Soft-sediment deformation structures in Lower Badenian (Middle Miocene) foreshore sands and their trigger mechanism (Carpathian Foredeep Basin, Czech Republic)

Slavomír NEHYBA

KEYWORDS

foreshore deposits
Lower Badenian
density gradient
paleoseismicity
liquefaction
fluidization

Department of Geological Sciences, Faculty of Science, Masaryk University, Kotlářská 2, 611 37 Brno, Czech Republic;
slavek@sci.muni.cz

Abstract

Soft-sediment deformation structures have been recently recognized within Lower Badenian deposits of the Carpathian Foredeep in the outcrop near Oslavany (Moravia, Czech Republic). The deformed unit is sandwiched between undeformed foreshore deposits. The lithology (medium to fine, fine and very fine grained sands and silty sands) of both the deformed and the undeformed units is very similar. The deformation structures have been grouped into two categories, i.e. contorted and intruded. The contorted structures consist of convolute folds, contorted lamina sets and pillow-shaped structures. Cusps, dish and pillar structures, and sandy flame structures represent the intruded structures. The deformation mechanism is interpreted to be due to liquefaction/fluidization, and the seismic activity in the area under study is assumed to have been the trigger mechanism.

Synsedimentäre Deformationsstrukturen in unverfestigten Sedimenten konnten in Ablagerungen des Unteren Badenium in der Karpatischen Vortiefe in einem Aufschluss bei Oslavany (Mähren, Tschechische Republik) gefunden werden. Die deformierte Einheit ist zwischen ungestörten Ablagerungen eingeschaltet. Sowohl die deformierten als auch die ungestörten Sedimente sind lithologisch ähnlich und bestehen aus mittel- bis feinkörnigen, feinkörnigen und sehr feinkörnigen Sanden sowie siltigen Sanden. Bei den Deformationsstrukturen wurden gedrehte („contorted") und eingedrungene ("intruded") Strukturen unterschieden. Zu den gedrehten Strukturen zählen „convolute folds" (eingerollte Falten), "contorted lamina sets" (verbogene laminierte Abschnitte) und "pillow-shaped structures" (polsterförmige Strukturen). Die eingedrungenen Strukturen setzen sich aus „cusps" (höckerförmige Strukturen), "dish and pillar structures" (schüssel- und säulenförmige Strukturen) und "sandy flame structures" (sandige Flammenstrukturen) zusammen. Die Deformation wird durch Fluidisierung der Sedimente erklärt. Als Auslösungsimpuls wird die seismische Aktivität in diesem Gebiet angenommen.

1. Introduction

Soft-sediment deformations are created in unconsolidated sediment and are relatively common in sandy sediments (Lowe, 1975, 1976; Van Loon, 2009; Owen and Moretti, 2011). Deformation often occurs rapidly, close to the surface, during or shortly after deposition. Soft-sediment deformation processes transform progressively with increasing pore-fluid pressure from plastic deformation to liquefaction and from liquefaction to fluidization (Lowe, 1975).

Numerous natural processes can induce soft-sediment deformations (Lowe, 1975). A number of them are external to the depositional environment (i.e. allogenic triggers, including seismicity, glaciation and thermal activity), whereas others are part of the depositional environment (i.e. autogenic triggers, including rapid deposition, impact of waves) (Owen et al., 2011; Owen and Moretti, 2011). Certain triggers are extreme events that represent geohazards, and analysis of the structures can contribute to the assessment of their recurrence intervals (palaeoseismic studies) (e.g. Allen, 1986; Jones and Omoto, 2000; Bowman et al., 2004; Taşgin et al., 2011). Seismites, sediments with earthquake-induced deformations have been recorded in numerous sedimentary environments (e.g. Seilacher, 1984; Owen, 1995; Rossetti, 1999; Montenat et al., 2007; Taşgin and Türkmen, 2009).

The aims of this contribution are: (1) to describe types of soft-sediment deformation structures (SSDS) in Early Badenian marine deposits in the Moravian part of the Carpathian Foredeep in an area where they were previously unrecognized,(2) to describe the processes recorded within these deposits, and (3) to discuss their probable trigger mechanism.

2. Geological Setting

The position of the locality is presented in Figure 1a (GPS location 49°06.820 N and 016°20.237 E) and a simplified geological map of the studied area is presented in Figure 1b.The studied Neogene deposits belong to the Moravian part of the Carpathian Foredeep (MCF). The MCF extends southwards to the Austrian Molasse Basin (the North Alpine Foreland basin) and eastwards to the Polish part of the Carpathian Foredeep. The MCF is a peripheral foreland basin bounded by a steep, tectonically active eastern margin formed by the overthrust front of the Western Carpathians and a gently sloping western margin that onlaps onto the crystalline of the Bohemian Massif and its Palaeozoic and Mesozoic sedimentary cover. Thrust loading resulting from the prograding Carpathian nappes indu-

ced flexural subsidence of the western margin of the Bohemian Massif. Several stages of evolution of the MCF resulted in a highly varied shape and extent of the basin due to the complicated evolution of thrusting in both the Eastern Alps and Western Carpathians, also as a result of the complex tectonic and geological history of the basement (Nehyba and Šikula, 2007). The deposition in the MCF began in the Egerian/Early Eggenburgian and continued in the area under study up to the Early Badenian (Brzobohatý and Cicha, 1993). The shift in the orientation of the compression vector of the Carpathian orogenic wedge from NNW-NW towards NNE-NE occurred during the Late Karpatian - Early Badenian (Kováč, 2000), which was connected with a significant reconstruction of the basin (Nehyba and Šikula, 2007). The Lower Badenian deposits of the MCF reveal a maximum thickness of more than 700 m (Nehyba et al., 2008) and are represented by coarse-grained deltas, coastal and shallow marine, lagoonal and deeper-marine deposits, together with restricted occurrences of algal and bryozoan limestones, calcareous sandstones and horizons of distal air fall tephra (Nehyba, 1997). Isolated relics of the Lower Badenian deposits can be found far to the west of the present extent of the preserved basin (Nehyba and Hladilová, 2004).

The studied outcrop at Oslavany represents a holostratotype of the Lower Badenian deposits (Cicha in Papp et al., 1978). The former sand pit is no longer active and the original extent of the profile (see Cicha in Papp et al., 1978) has been severely reduced. The presently exposed strata were interpreted as a product of deposition in foreshore and shoreface (clastic coast of the Early Badenian Sea/ “passive”margin of the foreland basin). Five lithofacies (Sl, Sr, Ss, Sp, and M) were recognised (Nehyba et al., 2009).

The microfauna indicates Middle Badenian (sensu Hohenegger et al., 2014) assemblages of the “Lower Lagenid zone” (Nehyba et al., 2009). Planktonic foraminiferal biostratigraphical correlation might be based on the co-occurrence of *Orbulina suturalis* and *Praeorbulina sicana* (sample OSL3), corresponding with the time span of 15.1-14.5 Ma (Wade et al., 2011). Because the reworking of *Praeorbulina sicana* cannot be excluded, the studied sediments may be younger. The calcareous nannoplankton assemblages can be correlated with the upper part of the NN5 Zone due to the occurrence of *Sphenolithus heteromorphus* and the absence of *Helicosphaera ampliaperta* and *Helicosphaera waltrans* (14.36-13.34 Ma; Abdul Aziz et al., 2008; Gradstein et al., 2012). This confirms the younger age of the sediments as 14.5 Ma and the reworking of *P. sicana*. The relative abundance of reworked calcareous nannoplankton was also recognised. Oligocene (*Cyclicargolithus abisectus*, *Reticulofenestra bisecta*) and Cretace-

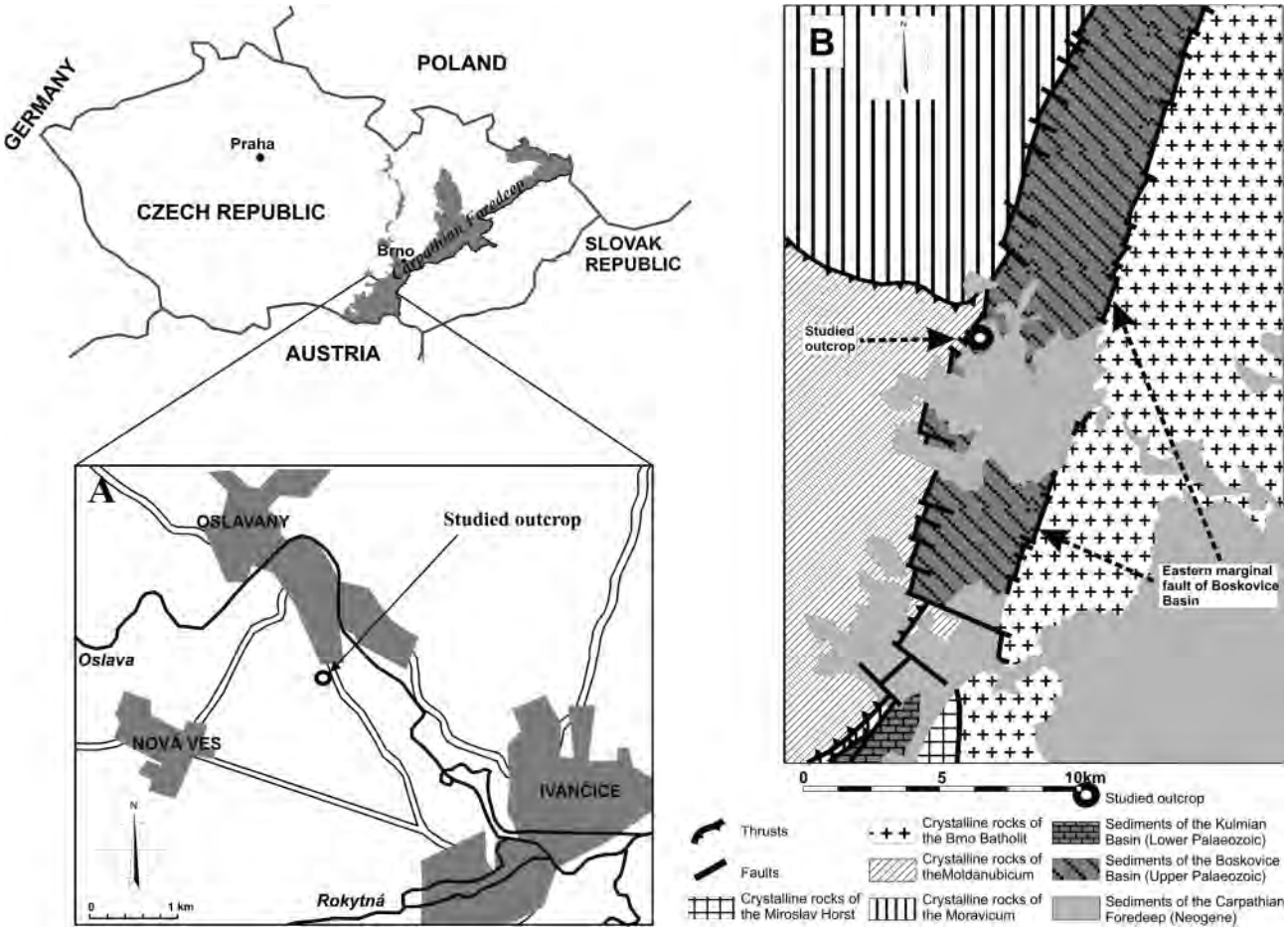

Figure 1: Location of the study area within the Carpathian Foredeep in the area of the Czech Republic. A) Simplified location map. B) Schematic geological map based on the geological map of the Czech Republic.

ous taxa (*Watznaueria* sp., *Arkhangelskiella* sp., *Micula* sp.) are the most common; occasionally Eocene *Chiasmolithus* sp. was also recorded. Among the planktonic foraminifera, Cretaceous *Globotruncana* sp. and the Early Miocene *Cassigerinella* occur rarely (Holcová et al., 2013).

3. Methods and Terminology

The sedimentary facies were studied using detailed logging, with local palaeocurrent directions following methods given by Walker and James (1992) and Nemec (2005). The grain size (18 samples) was analysed through the combined techniques of sieving and laser diffraction. Samples were systematically taken to demonstrate all facies and their grain-size variations. An AS 200 Fritsch sieve machine with a standard set of 7 sieves (4 mm-0.063 mm) was used for the analyses of the coarser grains and a Cilas 1064 laser diffraction granulometer for the finer ones (0.5-0.0004 mm). Ultrasonic dispersion, distilled water and washing in sodium polyphosphate were applied prior to the analyses in order to avoid flocculation of the analysed particles. The used grain size parameters were calculated according to Folk and Ward (1957).

A number of alternative names, definitions and classifications (e.g. Lowe, 1975; Van Loon, 2009; Owen et al., 2011) have been proposed for SSDS. They are classified here according to their morphology and deformation style, and grouped into two categories (i.e. contorted and intruded structures). The general term “contorted structures” is used for features with different degrees of crumpling or complicated folding of the laminae within the sand bed. The term “intruded structures” is used for structureless masses of sand displaying different styles of elongated shapes that have intruded into other deformed sand beds (Rossetti, 1999).

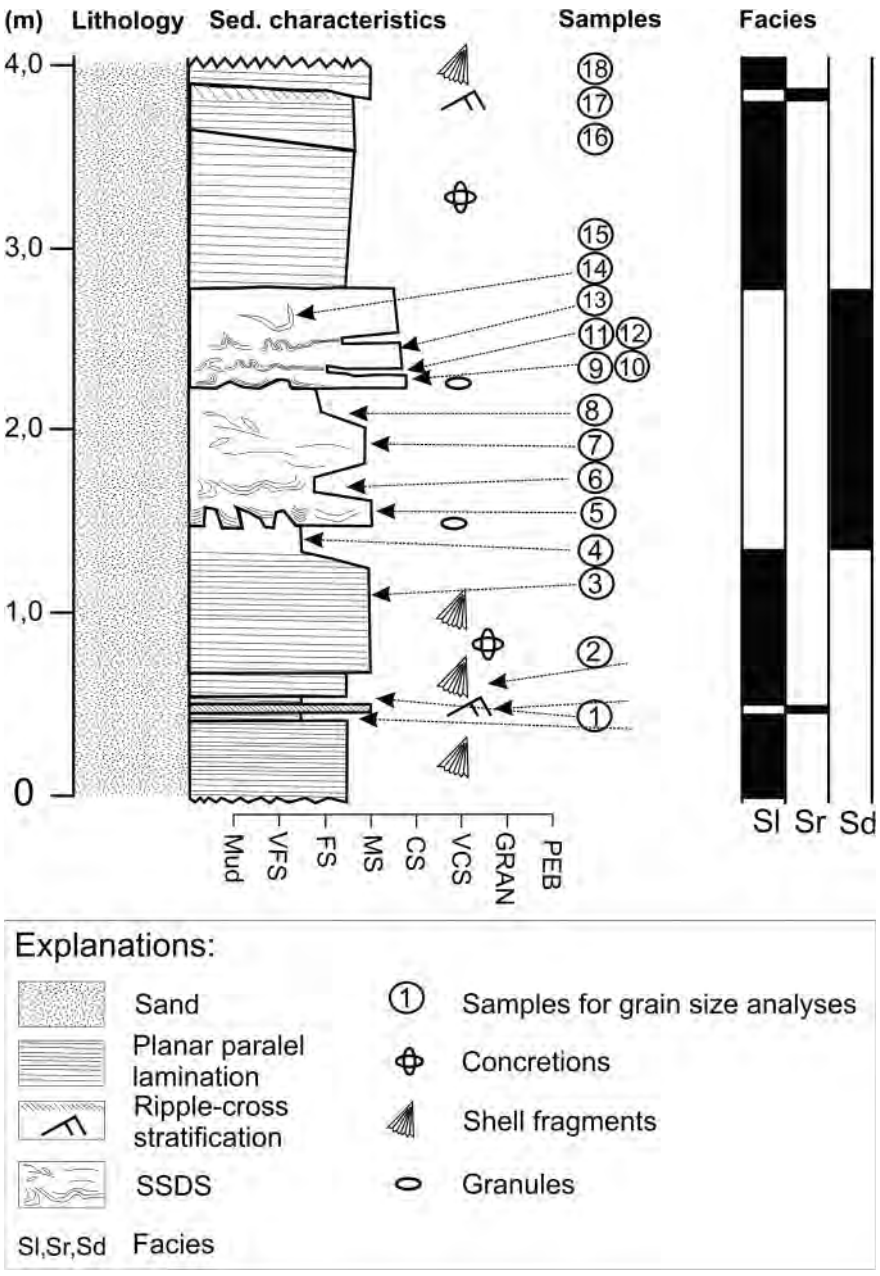

Figure 2: Schematic vertical log with the various lithofacies and position of all samples under study.

4. The Sedimentological Setting

The schematised vertical log with the recognized lithofacies is presented in Figure 2. The view of the wall of the sand pit in Oslavany with its deformed unit is presented in Figures 3 a, b. The grain size characteristics of the studied sands are presented in Table 1.

The undeformed unit consists mainly of tabular laminated beds of light yellow-brown sand to silty sand. Grain size differences occur at a decimetre scale. The planar parallel lamination, due to the alternation of slightly coarser- and finer-grained lamina, with coarser lamina richer in shell debris and with a low angle of inclination (max. 5°), represents the dominant Sl facies. The content of clay is very low (1.5 - 3%), whereas the silt content varies considerably (9.6% - 22.3%). Sands are very fine to fine, fine or fine to medium-grained, moderately well to poorly sorted and leptokurtic to very leptokurtic (samples 2, 3, 15, 16 and 18 in Table 1). The granule fraction is dominantly formed by shell fragments. Rare iron concretions (up to several centimetres in diameter), granules of schists and quartzes, and extremely rare small mudstone intraclasts (max. 1 cm) were also observed. The occurrence of rippled fine to very fine silty

sand of the Sr facies was rare in the profile, usually forming about 5 cm thick interbeds within the dominant beds of the Sl facies. A higher content of silt and clay, poorer sorting, mesokurtic and very leptokurtic kurtosis were recognized in the Sr facies (samples 1, 17 in Table 2) than in the Sl facies. The Sl and Sr facies were interpreted as foreshore deposits (Nehyba et al. 2009).

The deformed unit has a roughly planar shape with a maximum visible thickness of approx. 120 cm (Fig. 3A, B). Both the basis and the top of the unit are sharp. The basis is undulatory with a relief of up to 12 cm. The top is sharp and slightly inclined. Packages of undeformed sand occur below and above the deformed unit. The deformed unit is composed of two subunits. The lower subunit has a roughly tabular shape; its thickness ranges from 55 to 70 cm and can be traced along the whole outcrop over a distance of 15 m. The upper subunit has a wedge shape and it wedges out generally towards SE-ESE. The maximum thickness of the upper subunit was 73 cm and it can be traced to a distance of more than 10 m. The further lateral extent of both subunits is uncertain due to collapsed pit walls.

The deformed sands (Sd facies) are light yellow-brown and medium- to fine-grained. The contorted structures are represented here by convolute folds, contorted-lamina sets and pillow-shaped structures. These structures are surrounded by relatively coarser medium to fine, or fine sand; rarely silty sand; this sand is relatively well to poorly sorted, leptokurtic to very leptokurtic. The primary lamination may be partly preserved or homogenised (structureless). The silt content is usually low. The content of clay is particularly low (samples 7, 8, and 13 in Table 1).

Convolute folds (Fig. 4a-d) are represented by folded and contorted to distorted stratification, which forms laterally alternating convex- and concave-upward morphologies. In certain cases, the folds are upright and cuspate, with rounded synclines and sharper anticlines, while in other cases a more chaotic style prevails. These folds are 5-30 cm high and up to 60 cm wide. The spacing of wide synclines and narrow anticlines is relatively irregular. The shape, width, height, and orientation of the overturned parts often change laterally without any preferred orientation. The convolute folds are formed by fine to very fine silty sand, moderately to relatively poorly sorted and very platykurtic (samples 6 and 11 in Table 1). A very low content of medium and coarser sand is characteristic. The internal lamination and bedding, although distorted, is partly preserved, being parallel to the basal surface and bent upward towards the anticlines. The thickness of the folded layer is about 5 cm and several superimposed folded layers are present. They are surrounded by structureless sand with intruded structures. The convolute folds are generally coherent and do not increase in intensity (Jones and Omoto 2000) from the base to the top of the deformed unit. However, the convolute folds become diffuse laterally in the upper subunit, grading into almost undeformed undulated to planar parallel laminated silty fine to very fine sand (sample 12 in Table 1). This is related with the continuous thinning and final wedging out of the interbeds of the fine to very fine silty sand and also the wedging out of the upper subunit. No lateral variation in the intensity of deformation is present in the lower subunit.

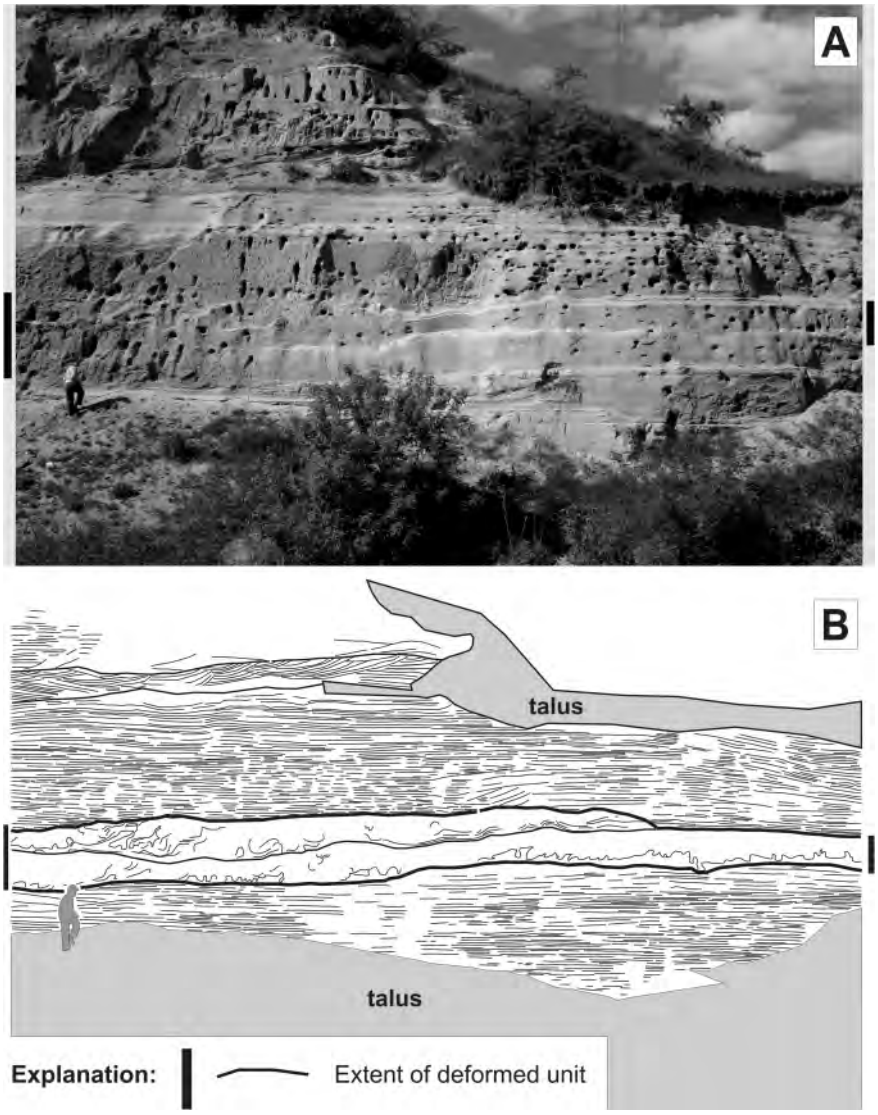

Figure 3: The sand pit at Oslavany. A) View on the wall (person for scale), B) Line drawing of the wall of sand pit Oslavany. Note that the deformed unit is sandwiched between undeformed beds of planar parallel laminated sand.

The contorted-lamina sets (Fig. 5a, b) typically exhibit contorted fine laminae with upturned margins. The alternation of slightly coarser laminas of medium and fine sand is characteristic. The structure is up to 50 cm long and 8-20 cm thick. Medium to fine sands and rarely silty sands are relatively poorly sorted, very leptokurtic (samples 5, 9 and 10 in Table 1). The occurrence of granules, a relatively higher content of coarse and very coarse sand, and a relatively lower content of silt and clay than in the adjacent intruded structures or convolute folds are typical for the sands with contorted-lamina sets. This disrupted bedding is typically present in the superposition of cusps.

The pillow-shaped structures (Fig. 6A, B) are characterised by broad synclinal morphologies. They are formed by fine to very fine silty sands, poorly sorted and very platykurtic (sample 14 in Table 1) with a slightly increased silt content. The individual synclines are usually asymmetrical (without any preferred orientation) and partly overturned, ranging from 5 to 20 cm in width and they are maximally 10 cm high. The thickness of the deformed sand layer is usually only a few centimetres. The structures are internally almost massive with extremely poorly preserved internal laminae that are conformable with the synclinal shape. A complete loss of structure continuity and "floating" structured parts within the surrounding "host" of coarser fine to medium structureless sand with intruded structures are typical.

The intruded structures consist of cusps, dish and pillar structures, and sandy flame structures. They were all identified within generally structureless slightly coarser sands, partly (dish and pillar structures, sandy flame structures) in superposition of sands with contorted structures.

The cusps consist of short upward curved protuberances of relatively finer sand into relatively coarser sand along the sharp boundaries between two sand layers. They are columnar, generally straight and vertical, sometimes morphologically similar to large flame structures, although the cusps represent masses of underlying deformed sands that intrude into the overlying sand beds. The cusps consist of fine silty sand, moderately well sorted and very leptokurtic (sample 4 in Table 1). The height of the cusps varies between 5 and 20 cm; they are up to 15 cm wide and internally structureless (Figs. 5a-d, 6c, d). They protrude into fine- to medium-grained silty sand, very poorly sorted and very leptokurtic (sample 5 in Table 1). These sands are either structureless or exhibit con-

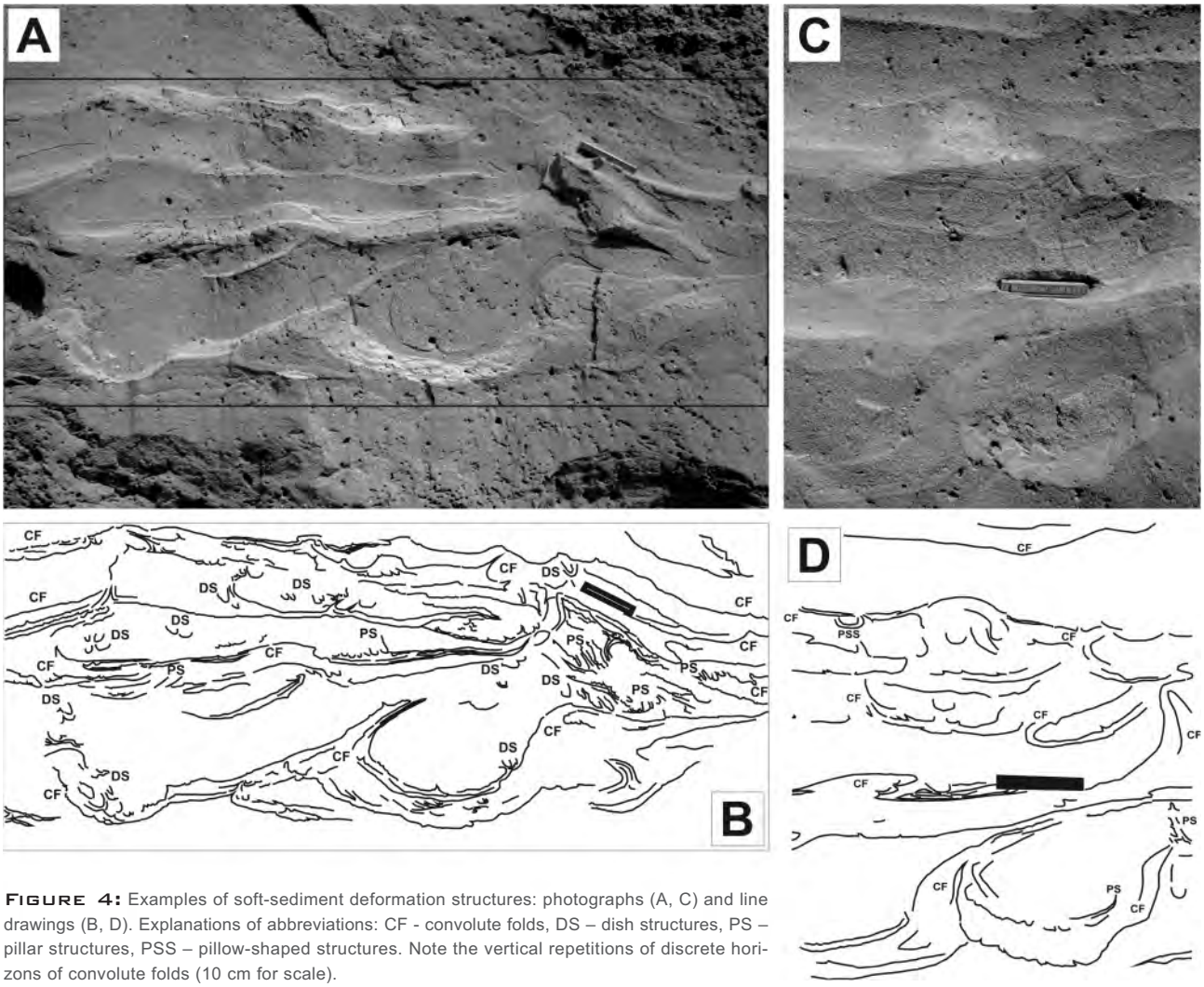

Figure 4: Examples of soft-sediment deformation structures: photographs (A, C) and line drawings (B, D). Explanations of abbreviations: CF - convolute folds, DS – dish structures, PS – pillar structures, PSS – pillow-shaped structures. Note the vertical repetitions of discrete horizons of convolute folds (10 cm for scale).

torted-lamina sets. The principal difference between protruding sand forming cusps and the sand around it is in the relative proportion of fine and very fine sand, and medium, coarse and very coarse sand, whereas the content of silt and clay is very similar (see samples 4 and 5 in Table 1).

The dish structures are small (several cm thick and long) structures reflecting the upward escape of pore water (Fig. 4, 6e, f). The dishes are concave upward features, roughly equidimensional in shape, typical for a relative enrichment of finer sand within the coarser sand.

The pillar structures consist of discrete, subvertically elongated to slightly sinuous paths (Figs. 4-6) enriched with relatively finer sand. The pillars are up to 8 cm long and less than 3 cm wide. They are present in the superposition of cusps or convolute folds, isolated or irregularly grouped, and locally form bifurcated paths.

The sandy flame structures are small scale structures, which look like thin sandy irregular dykes and sills. They are up to 10 cm long and up to 2 cm thick, sometimes terminated by irregular lenses, which are up to 3 cm long and about 2 cm high (Fig. 5). Sandy flame structures are composed of fine to very fine silty sand within slightly coarser host sand. They are often situated above or close to the disrupted anticlines of the convolute folds, or to cusps (Fig. 5 c, d). The structure often laterally changes their shape, length and height, as well as the orientation, but orientation generally parallel to the bedding seems to be most common.

The vertical succession of cusps-contorted lamina sets-convolute folds and structureless sands with pillow-shaped structures, dish and pillar structures and sandy flame structures could be generally followed in both subunits from their bases to the tops. Structureless sands are also present above the cusps and contorted lamina sets.

5. The Deformation Mechanism

The deformation mechanism of SSDS must be determined correctly for a reliable reconstruction of the trigger (Allen, 1986; Owen, 1987; Maltman and Bolton, 2003). Several processes may act together during the deformation (Lowe, 1975; Rossetti, 1999). Similarly, several possible explanations exist for the genesis of SSDS.

The studied SSDS were formed in loose, unconsolidated water-saturated foreshore sands. The lithological similarity between the deformed and undeformed sediments is clear (see Table 1). The original stratification and bedding were folded, disrupted or even totally destroyed (homogenised), with new structures being generated. The deformation occurred in-place without substantial lateral transport. The intensity of deformation within the deformed unit varied. The wedging out of the upper deformed subunit and lateral variations in the intensity of deformation in this subunit are related to the wedging out of the thin interbeds of very fine to fine silty sand within coarser medium to fine sand. This observation points to a principal role of the initial multi-layered succession with the superposition of thicker beds of coarser medium to coarse sand ("relatively heavy") on thinner beds of finer very fine to fine silty sand ("relatively light"). This is a driving force system (Owen, 1987) related to a gravitational instability, in the form of a reversed density gradient (Moretti and Ronchi, 2011). In each reversed density system, the heavier sands may sink into the lighter sands and silts, accompanied by a drastic decrease or complete loss of the shear strength of the sediments (Allen, 1982; Owen, 1987; Moretti and Ronchi 2011). The deformation of the primary lamination shows that the decrease of shear strength was induced by liquidization. This is further supported by the association of SSDS (more and less liquefied or fluidized sands) and by the absence of mud

Sample	Facies	Granules (%)	VCS (%)	CS (%)	MS (%)	FS (%)	VFS (%)	Silt (%)	Clay (%)	Mz (Φ)	sI (Φ)	Kg
1	Sr	-	-	0.8	9.5	35.9	27.3	22.3	4.1	3.8	1.8	1.0
2	Sl	-	1.7	11.5	40.8	36.5	8.4	9.6	1.5	2.2	1.3	1.46
3	Sl	0.01	0.01	1.2	30.8	42.4	12.0	12.5	1.3	2.6	1.3	1.61
4	Sd	-	0.1	0.9	29.9	51.7	17.4	11.2	2.4	2.6	1.3	1.98
5	Sd	-	0.02	0.05	4.4	52.4	22.2	19.0	2.0	3.4	1.4	0.41
6	Sd	0.8	6.3	12.9	34.7	37.3	8.8	11.1	2.6	2.5	2.6	1.84
7	Sd	-	0.8	8.1	38.0	36.2	7.8	8.1	1.0	2.2	1.2	1.36
8	Sd	-	0.1	0.6	5.6	71.2	22.5	14.7	3.5	3.4	1.6	1.91
9	Sd	-	0.2	1.0	10.8	35.5	29.5	19.7	3.3	3.6	1.7	0.49
10	Sd		0.1	1.2	18.1	45.7	35.0	17.8	3.6	3.6	1.8	1.68
11	Sd	0.6	4.8	13.1	29.1	25.2	10.2	13.9	3.1	2.7	2.1	1.60
12	Sl	1.5	7.6	6.6	32.6	48.0	8.9	7.3	1.5	2.17	1.3	1.80
13	Sd	0.6	3.8	6.2	30.2	40.1	8.2	9.4	2.0	2.3	1.5	1.90
14	Sd	-	-	0.1	6.6	47.8	31.7	17.6	2.9	3.6	1.6	0.46
15	Sl	-	0.4	4.5	23.8	40.3	31.0	16.7	3.4	3.2	1.8	1.51
16	Sl	0.05	4.8	18.0	38.2	30.7	14.5	12.3	3.0	2.4	1.8	1.50
17	Sr	-	-	0.5	11.4	47.0	41.1	17.9	4.2	3.7	1.9	2.01
18	Sl	0.03	1.7	6.4	25.5	51.4	15.0	10.7	2.4	2.6	1.5	2.23

Table 1: Grain size characteristics of samples of the studied Lower Badenian deposits. Explanations of abbreviations: VCS – very coarse sand, CS – coarse sand, MS – medium sand, FS – fine sand, VFS – very fine sand, Mz – average grain size/mean, σI – dispersion/sorting, Kg – kurtosis, Φ - phi value.

layers in the succession (Owen, 1996b; Rossetti, 1999). The observed cusps, convolute folds, pillow-shaped structures and sandy flame structures are formed in very fine to fine silty sands, whereas the contorted lamina sets and structureless sands are connected with coarser medium to fine sands. Liquidization is most likely to develop in loosely packed water-saturated deposits of well sorted coarse silt to medium sand grain size with low cohesion (Mills, 1983; Obermeier, 1998; Moretti et al., 1999; Owen and Moretti, 2011). Such sediments might lose cohesion and liquefy, following an excess of pore pressure under water-saturated conditions.

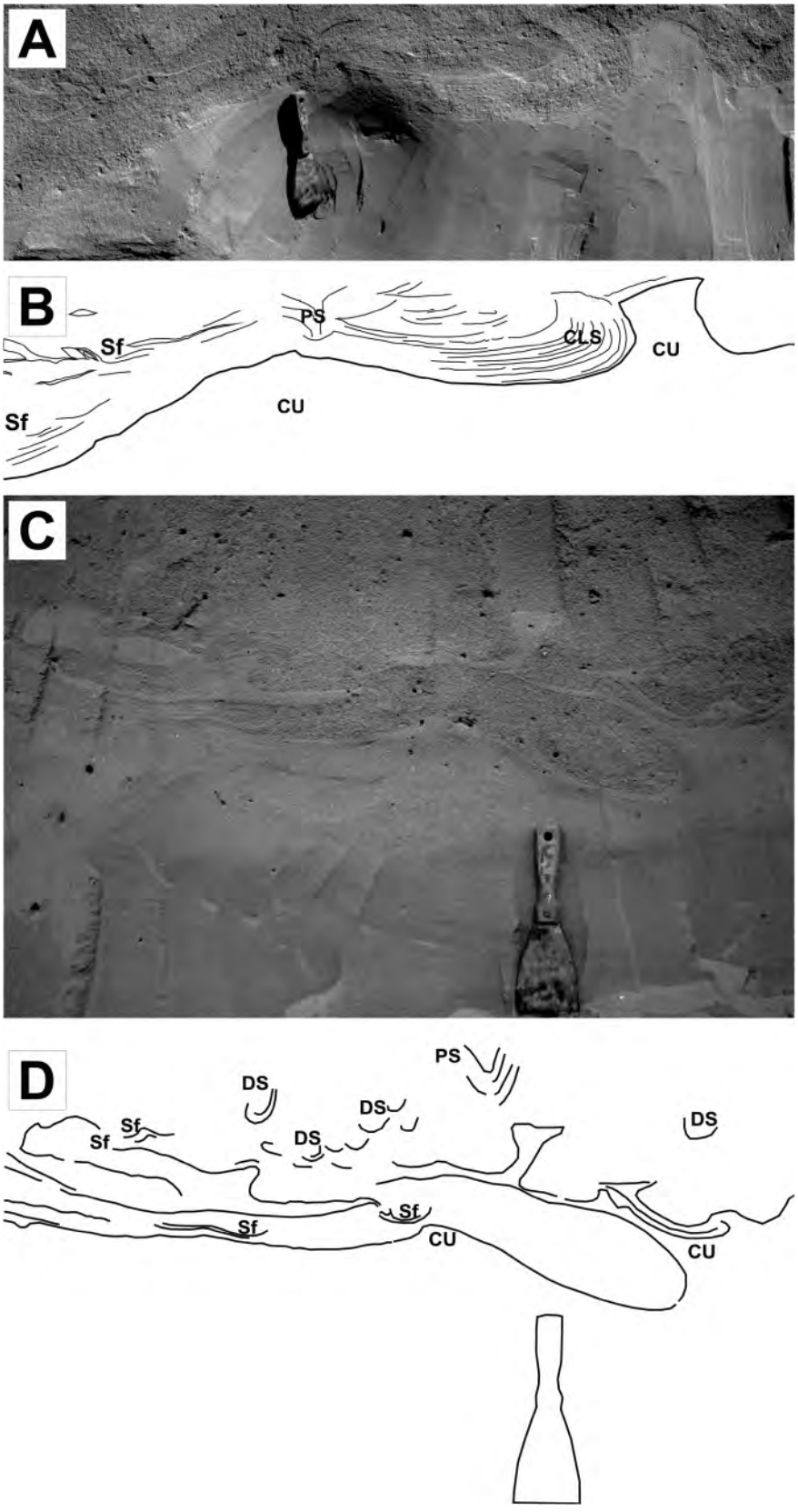

Figure 5: Examples of soft-sediment deformation structures: photographs (A, C) and line drawings (B, D). Explanations of abbreviations: CLS – contorted-lamina sets. CU – cusps, DS – dish structures, PS – pillar structures, Sf – sandy flame structures (Spatula for scale).

The contorted structures indicate limited particle movement, which deformed the primary structure without obliterating it (cf. Lowe, 1975). The preservation of lamination demonstrates that the sands did not undergo turbulence during liquefaction, but rather remained coherent to semi-coherent. Massive structureless beds of sand may reflect a longer duration of the liquidized state and full support of the grains in the fluid (fluidization). Fluidization, which is capable of separating grains according to their particle size, is a more likely cause of the loss of the primary structures and the elutriation of finer grains (Collinson et al., 2006). The association of contorted and intruded structures points to limited upward and sideward flowage of sediment and water.

Further supporting evidence for liquidization includes: a) the pervasive, ductile character of the SSDS (cf. Bryant and Miall, 2010); b) the partial preservation of stratification (cf. Doe and Dott, 1980; Owen, 1987); and c) the upward variations in the degree and complexity of deformation in the deformed subunits (Moretti et al., 1999; Owen, 1996b). Van Loon and Wiggers (1976) attributed deformation units with remnants of vaguely bedded parts to “false-body thixotropy”.

The water-escape features can be directly related to gravitational readjustment (upward-directed movement of underlying light sands), and/or it can be the result of beds with different selective fluidization processes

arising from the restoration of grain-supported packing after complete liquefaction (Allen, 1982; Owen, 1987; Moretti et al., 1999).

The final morphology of the interface between two layers with a reversed density gradient is related to several parameters (e.g. the dynamic viscosity, the duration of the liquefied state,…) nevertheless, this interface generally is deformed in a more or less regular way (Moretti and Ronchi, 2011). However, the studied structures are irregular, varying laterally in size and morphology. This can be explained by the lateral variations in the thickness of the beds and by the different kinds of lamination (i.e. planar parallel lamination, ripple cross-lamination) that induce the irregular distribution of packing and porosity in the initial multi-layered unstable density system. Such a complex initial sedimentary column implies the action of another possible driving force system during and after liquefaction, this is called unequal loading by Allen (1982).

A simplified model of the formation of the SSDS under study is presented in Figure 7. The explanation for the differential liquefaction or fluidization of the studied sediment is connected with contrasting packing and porosity between adjacent layers, which cause potentially instability and susceptibility to deformation (Maltman, 1994). The formation of the initial multi-layered succession is the result of fluctuations in the current power and variations in depositional rates. The result is the formation of a vertical succession of foreshore deposits with

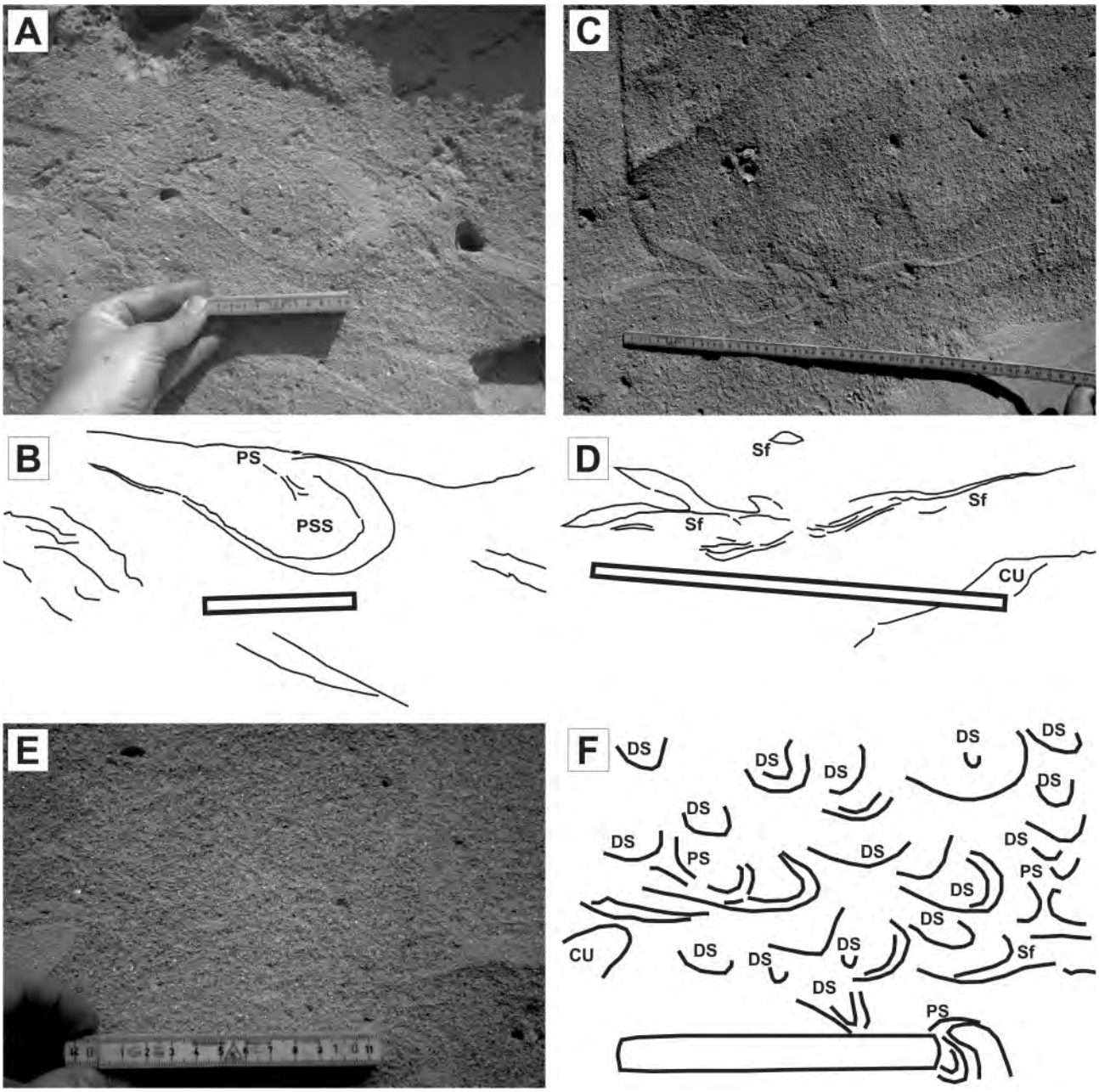

Figure 6: Examples of soft-sediment deformation structures: photograph (A, C, E) and line drawing (B, D, F). Explanations of abbreviations: PSS – pillow-shaped structures, PS – pillar structures, DS – dish structures, CU – cusps, Sf – sandy flame structures (10 cm for scale in A, B, 40 cm for scale in C, D).

alternations between (A) thicker beds of better sorted, coarser-grained, leptokurtic medium to fine sand with an admixture of coarser grains and a very low content of silt, and (B) thinner interbeds of less sorted, finer-grained, mesokurtic to leptokuric fine to very fine silty sand (Fig. 7a). In other words, thinner beds with a closely packed framework, lower initial porosity and lower potential for instability alternate with thicker less-closely packed beds with a higher initial porosity and a higher potential for instability. Such a situation led to the differential liquefaction or fluidization of adjacent beds and to the complexity of the SSDS.

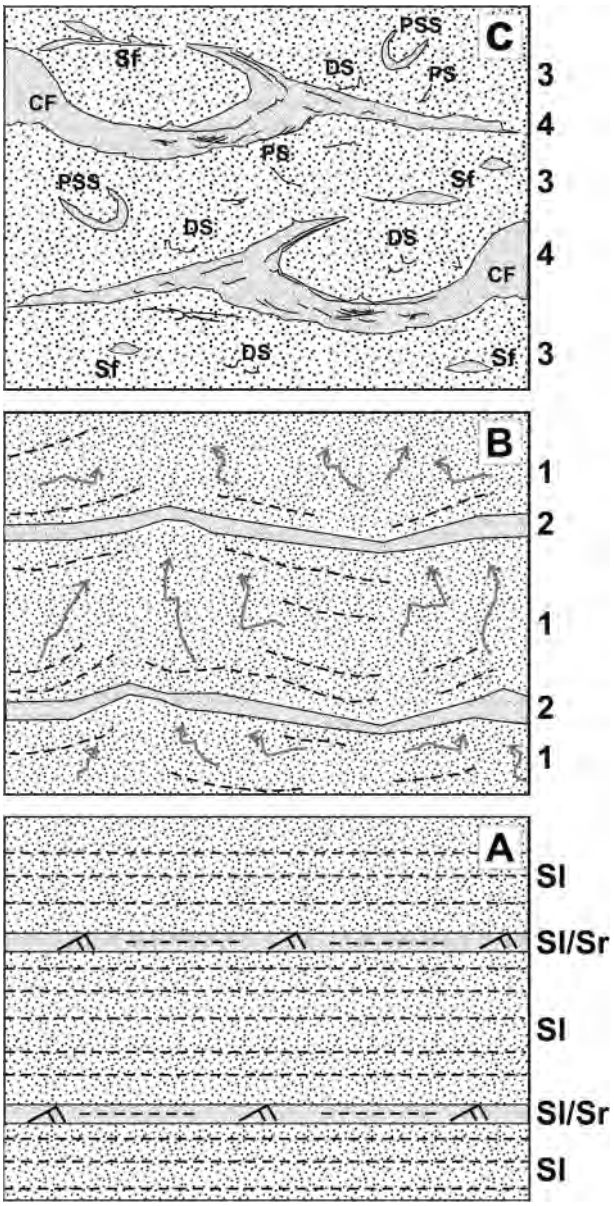

Figure 7: Schematic model of the formation of soft-sediment deformation structures in the studied sediments. A) Starting conditions with an alternation of thicker beds of medium to fine grained sand with planar parallel stratification (Sl) and thinner interbeds of fine to very fine silty sand with planar parallel or ripple lamination (Sl/Sr), B) Starting liquefaction of sandy beds with different rheological behaviour (1 and 2). Contorted lamina sets are formed within the more liquidized thicker beds of coarser, better sorted coarser sands, whereas folding started to deform less liquidized thinner beds of the finer grained, poorly sorted silty sand, C) final state of the deformation - intruded structures within more liquidized beds of structureless coarser sand (3) and convolute folds represent the dominant structure of less liquidized beds of finer sand (4). Explanations of abbreviations: CF - convolute folds, DS – dish structures, PSS – pillow-shaped structures, PS – pillar structures, Sf – sandy flame structures.

Liquidization generated a contrast between these sandy beds with different rheological behaviour, which finally led to the formation of a deformed unit where intruding structures are present in structureless coarser sand and where convolute folds represent the dominant structure of discontinuous beds of finer sand (Fig. 7b, c). The convolute folds were formed when less liquefied, thus more compacted sediment sank to replace the underlying sand removed by fluidization. As the deformation became more pronounced, sandy flame structures or pillow-shaped structures were formed. Irregular convolute folds are probably related to more intense/liquefied sediments due to their pronounced deformation. The contorted-lamina sets were formed where liquefied sediment replaced the underlying sand that was removed by the liquidization of associated structureless beds. The associated massive sands represent the lowest degree of sediment compaction and the most intense liquidization/fluidization (Rossetti, 1999). The sinking parts of beds were accompanied by simultaneous upward, or even sideward, flowage of water and sediment. Cusps, dish and pillar structures are interpreted as representing flow paths with fluidized sediments that were injected from the surrounding strata as a result of increasing interstitial pore pressure (Owen, 1996a). Cheel and Rust (1986) described dish structures as the last of a series of liquefaction products.

6. The Trigger Mechanism

Most deformation mechanisms are initiated by the action of a “trigger.” Many natural agents and processes can act as a trigger for liquidization in a foreshore setting (Owen and Moretti, 2011). There is no direct and simple relationship between the type of soft-sediment deformation and the triggering agent, due to the principal role of the driving force and initial sedimentary succession. Moreover, more than one trigger mechanism tend to occur in a given deformation episode (Shiki, 1996; Jones and Omoto, 2000). However, the analysis of sedimentological features in the entire succession can be a useful tool to distinguish between the possible triggers (Moretti and Ronchi, 2011).

The results of the sedimentological study of the deformed and undeformed units of the Oslavany outcrop show that: (1) deformation is induced by liquidization in a multi-layered succession with initial unstable density gradients; (2) deformation involves marine foreshore deposits; (3) deformation is absent in the beds that are located below and above the disturbed bed; and (4) deformed and undeformed beds show similar lithologies and sedimentary fabric (especially sedimentary textures). The last two properties point to an external trigger. Seismic shocks are thought to be the trigger of liquefaction and fluidization in the studied case. Seismites, sedimentary layers with earthquake induced deformations, have been recorded in numerous sedimentary environments (e.g., Seilacher,

1984; Owen, 1995; Rossetti, 1999; Montenat et al., 2007; Taşgin and Türkmen, 2009), although they were only recently found in the Lower Badenian of the MCF.

The more or less generally accepted seismite criteria (Jones and Omoto, 2000; Montenat et al., 2007; Hilbert-Wolf et al., 2009; Owen and Moretti, 2011) are:

1) Association with one or more faults likely to have been active during sedimentation. Although numerous faults were recognized in the area under study (see Fig. 1b), the most suitable fault for the production of high-magnitude earthquakes is the Eastern Marginal Fault of the Boskovice Basin, located approx. 3 km E of the outcrop. The fault has a SSW-NNE orientation and a length of more than 40 km. This structure separates the principal geological units of the Bohemian Massif, i.e. the Moldanubian unit, the Moravian unit, the Letovice and Zábřeh Crystalline Complexes to the West; the Brno Massif and Moravo-Silesian Palaeozoic deposits (Culm facies) to the East. The Boskovice Basin (an extensional basin/half graben), with a more than 3 km thick Permo-Carboniferous sediment infill, was formed along this fault (Nehyba et al., 2012). Significant differences in the thickness, preservation, stratigraphy and facies of the Neogene deposits of the MCF occur along the eastern margin of the Boskovice Basin. Quaternary tectonic activity of the area described Leichmann and Hejl (1996) and Roštínský et al. (2013). All these observations point to important and long-term activity of the fault, therefore such activity may well have taken place also during the Early Badenian.
2) The observed deformation should be consistent with deformations with a known seismic origin. The SSDS under study are all well comparable with SSDS reported from the geological record that were induced by earthquakes (Bowman et al., 2004; Mazumder et al., 1998a, b; Ross et al., 2011; Moretti et al., 1999), as well as with those produced experimentally (Seilacher, 1984; Nichols et al., 1994; Owen, 1996b; Scott and Price, 1988). However, experiments have shown that the SSDS morphology depends on the initial sediment conditions and driving forces, rather than on the liquefaction trigger (Jones and Omoto, 2000).
3) The criterion of widespread occurrence of deformation structures and the criterion of lateral continuity of the horizons with seismically triggered SSDS (Hibert-Wolf et al., 2009) are difficult to apply in such a poorly exposed area as the MCF. Furthermore, the criteria have some critical points: Greb and Archer (2007) and Alfaro et al. (2010) demonstrate how seismically deformed beds can disappear laterally as a result of thickness changes and/or lateral facies variations. The lower deformed subunit has been followed over a distance of about 15 m. Further tracing was impossible due to collapse of the walls of the sand pit. The upper subunit is not continuous, which is connected with the wedging out of interbeds of silty very fine sand within relatively coarser fine sand, and thus also with the disappearence of the initial unstable density gradient. The limited lateral extent of the upper subunit bed can be explained in this way.
4) The exclusion of other potential causal mechanisms is a further criterion. The main triggers for liquefaction-induced SSDS in the foreshore environment include: (1) pressure fluctuations associated with water waves, in particular storm waves (Alfaro et al., 2002; Molina et al., 1998; Owen, 1987); (2) the impact of breaking water waves (Dalrymple, 1979, 1980); (3) tsunamis (Matsumoto et al., 2008); and (4) rapid sediment accumulation and sediment loading (Oliveira et al., 2009; Postma, 1983). Studies which have inferred the action of a non-seismic trigger have either noted the absence of evidence for a seismic trigger or used an assessment of the overall sedimentological and palaeoenvironmental context.

   The deformed unit is about 1.2 m thick and continuous on the outcrop scale; the deformation involves well-defined generally horizontal beds with various kinds of lamination reflecting different depositional conditions. There is no evidence of mass deposition, nor was there the significant forward displacement of sediment. This excludes a slope related gravity flow origin of the SSDS, thus the high instantaneous sedimentation rate can be excluded as a trigger. Common criteria for strong oscillatory flows such as storm waves are bedforms such as hummocky cross-stratifications and symmetrical ripples (Sherman and Greenwood, 1989; Cheel and Leckie, 1993), or isolated slump bodies on the upper stoss side of mega-ripples (Dalrymple, 1979). These structures and bedforms were not identified in the studied sedimentary succession. This also holds for the erosional and depositional evidence that might indicate "tsunamiites" (Dawson and Stewart, 2007).

   Molina et al. (1998) reported casts and isolated water escape structures due to storm waves. The SSDS under study are not isolated; they show a wide variety of structures. Moreover, no differences were recognised in the composition of benthic foraminiferal assemblages, especially when comparing samples from deformed and undeformed units (Holcová et al. 2013).
5) A cyclic repetition of deformed layers is expected in seismic zones as a result of successive seismogenic triggers. Although only one deformed unit, divided in two subunits, occurs in Oslavany, the vertical repetitions of discrete horizons bearing similar SSDS were identified within both subunits.
6) A key criterion in determining the action of an allogenic trigger is the presence of undeformed beds, identical in lithology and facies to the deformed horizon above and below it (Moretti and Ronchi, 2011). The deformed unit sandwiched between undeformed deposits and lithological and facies similarities are present, indeed, in the studied case. Sims (1975) and Wheeler (2002) mentioned several additional criteria for deformation features of seismic origin, i.e. A) evidence of sudden formation; B) evidence of synchroneity; and C) exhibition of a zoned distribution. The occurrence of SSDS in both subunits in Oslavany demonstrates at least approximate synchroneity of their formation, and

their abundance provides evidence of the suddenness of formation.

7. Discussion

The SSDS under study are the first described physical evidence of seismic activity along the passive margin of the MCF during the Early Badenian. Seismically-induced deformations have also been described in the Ukrainian part of the Carpathian Foredeep Basin (Wysocka et al., 2012). The passive margins of the peripheral foreland basins are often subjected to the synsedimentary reactivation of basement faults (Baumont, 1981; Gupta, 1999). The existence of numerous isolated relics of Lower Badenian deposits (Nehyba and Hladilová, 2004) with evidence of relatively deep marine conditions (Brzobohatý, 1997; Zágoršek et al., 2009) preserved on the foreland of the MCF and oriented almost linearly in the NW-SE direction (almost perpendicular to the basin axis) often along the basement fault reflect such a situation.

The earthquake magnitude was large enough to produce a significantly enhanced pore pressure leading to sediment deformation (cf. Hilbert-Wolf et al., 2009). The magnitude of the seismic events can be roughly estimated by examination of trends of liquefaction versus the epicentral distances of modern earthquakes (Galli, 2000). Liquefaction is unlikely to have developed in earthquakes of a magnitude of less than 5, and earthquakes of a higher magnitude may have triggered liquefaction over a wider area (Allen, 1986; Galli, 2000). A magnitude of less than 5 causes little or no liquefaction beyond a radius of 4 km; at a magnitude of 7, there is little or no liquefaction beyond a radius of 20 km (Scott and Price, 1988; Jones and Omoto, 2000; Taşgin and Tűrkmen, 2009). The Eastern Marginal Fault of the Boskovice Basin is located at a distance of approx. 3 km E of the outcrop. The fault shows a SSW-NNE orientation and a length of more than 40 km. Further evidence of seismic activity along this fault might be hidden within the Neogene or possibly Quaternary deposits in the area. This may help determine the recurrence intervals of a major seismic event, as well as the risk assessment and the reconstruction of the long-term patterns of seismicity in the study area. According to Owen and Moretti (2011), the extrapolation of the relationship between earthquake magnitude and distance to the farthest liquefaction effects indicates that extremely infrequent, very high-magnitude earthquakes could liquefy susceptible deposits across an entire sedimentary basin. Wagreich et al. (2008) supposed Early/Mid Badenian earthquake induced gravity flows in the Vienna Basin. Intense seismic activity in the Vienna basin could also led to deformation of the deposits of the MCF.

Due to the relationship between earthquake energy and the intensity of soft-sediment deformation, attempts have been made to develop soft- sediment deformation scales to qualitatively measure soft- sediment deformation, hence earthquake energy. The studied structures can be compared with categories 3 and 4 of the semi-quantitative seismite intensity scale of Hilbert-Wolf et al. (2009).

8. Conclusions

Soft-sediment deformation structures have been newly described in the Lower Badenian (the upper part of the NN5 Zone) marine deposits of the Moravian part of the Carpathian Foredeep in the Oslavany outcrop. The deformed unit is sandwiched within undeformed foreshore deposits. Light yellow-brown, medium to fine sand or very fine to fine silty sand with planar parallel stratification (low angle of inclination - up to 5°) form the absolute dominant facies of the undeformed beds. Facies of rippled and slightly finer grained sand is notably less common.

The deformed unit reveals a maximum thickness of approximately 120 cm and consists of sands with lithological characteristics similar to the undeformed ones. The deformation structures under study were grouped into two categories- contorted and intruded. Convolute folds, contorted lamina sets, pillow-shaped structures, cusps, dish and pillar structures, and sandy flame structures represent individual soft-sediment deformation structures. The varied intensities of liquidization and of the resulting soft-sediment deformation are due to the initially unstable multilayered succession. This was due to: i) an alternation of thicker beds of medium to coarse sand and beds of finer very fine to fine silty sands; ii) lateral variations in the thickness of beds; and iii) the irregular distribution of packing and porosity in the various kinds of lamination (planar parallel lamination, ripple cross-lamination).

The structures were produced by liquefaction and/or fluidization of unconsolidated sand. The passage of seismic wave (an earthquake trigger) is the most likely cause of the deformation. Such earthquake had probably magnitude above 5. The existence, association and depositional settings of the soft-sediment deformation structures attest to the tectonic activity in this area during the Early Badenian.

Acknowledgements

The author wishes to thank the Grant Agency of the Czech Republic No. 205/09/, which kindly sponsored the costs of the analytical data and part of the field work. He is also very grateful to R.Roetzel, T.van Loon, M.Wagreich and an unknown reviewer for all critical and stimulating comments, which highly improved the quality of the manuscript.

References

Abdul Aziz, H.A., Di Stefano, L.M., Foresi, F.J., Hilgen, S.M., Iaccarino, K.F., Kuiper, F., Lirer, G., Salvatorini, A. and Turco, E., 2008. Integrated stratigraphy and $^{40}Ar/^{39}Ar$ chronology of early Middle Miocene sediments from DSDP Leg 42A, Site 372 (Western Mediterranean). Palaeogeography, Palaeoclimatology, Palaeoecology, 257, 123-138.

Alfaro, P., Delgado, J., Estévez, A., Molina, J.M., Moretti, M. and Soria, J.M., 2002. Liquefaction and fluidization structures in Messinian storm deposits (Bajo Segura Basin, Betic Cordillera, southern Spain). International Journal of Earth Sciences, 91, 505-513.

Alfaro, P., Gibert, L., Moretti, M., García-Tortosa, F.J., Sanz de Galdeano, C., Galindo-Zaldívar, J. and López-Garrido, A.C., 2010. The significance of giant seismites in the Plio-Pleistocene Baza palaeo-lake (S Spain). Terra Nova, 22, 172-179.

Allen, J.R.L., 1982. Sedimentary structures: their character and physical basis, Vol. II. Elsevier, New York. 663 pp.

Allen, J.R.L., 1986. Earthquake magnitude-frequency, epicentral distance, and soft sediment deformation in sedimentary basins. Sedimentary Geology, 46, 67-75.

Beaumont, C., 1981. Foreland basins. Geophysical Journal of the Royal Astronomical Society, 55, 291-329.

Bowman, D., Korjenkov, A. and Porat, N., 2004. Late Pleistocene seismites from Lake Issyk-Kul, the Tien Shan range, Kyrgyzstan. Sedimentary Geology, 163, 211-228.

Bryant, G. and Miall, A.D., 2010. Diverse products of near-surface sediment mobilization in an ancient eolianite: outcrop features of the early Jurassic Navajo Sandstone. Basin Research, 22, 578-590.

Brzobohatý, R., 1997. Paleobathymetry of the Lower Badenian (Middle Miocene, Carpathian Foredeep, South Moravia) based on otoliths. In: Hladilová Š. (ed.): Dynamika vztahů marinního a kontinentálního prostředí, 37-45, Masarykova univerzita, Brno.

Brzobohatý, R. and Cicha, I., 1993. The Carpathian Foredeep. In: Přichystal, A., Obstová, O. and Suk, M. (eds.) Geologie Moravy a Slezska. Moravské zemské muzeum a Sekce geologických věd PřF MU, 123-128. Brno. In Czech.

Cheel, R.J. and Leckie, D.A., 1993. Hummocky cross-stratification. Sedimentological Revue, 1, 103-122.

Cheel, R.J. and Rust, B.R.,1986. A sequence of soft-sediment deformation (dewatering) structures in Late Quaternary subaqueous outwash near Ottawa, Canada. Sedimentary Geology, 47, 77-93.

Collinson, J., Mountney, N. and Thompson, D., 2006. Sedimentary Structures. 3rd edition, Terra Publishing, 291pp.

Dalrymple, R.W., 1979. Wave-induced liquefaction: a modern example from the Bay of Fundy. Sedimentology, 26, 835-844.

Dalrymple, R.W., 1980. Wave-induced liquefaction: an addendum. Sedimentology, 27, 461.

Dawson, A.G. and Stewart, I., 2007. Tsunami deposits in the geological record. Sedimentary Geology, 200, 166-183.

Doe, T.W. and Dott, R.H., 1980. Genetic significance of deformed cross-bedding – with examples from the Navajo and Weber sandstones of Utah. Journal of Sedimentary Petrology, 50, 793-812.

Folk, R. L. and Ward, W., 1957. Brazos River bar: a study in the significance of grain-size parameters. Journal of Sedimentary Petrology, 27, 3-26.

Galli, P., 2000. New empirical relationships between magnitude and distance for liquefaction. Tectonophysics, 324, 169-187.

Gradstein, F.M., Ogg, J.G., Schmitz, M.D. and Ogg, G.M.. 2012. The Geologic Time Scale 2012. Elsevier, 1176 pp.

Greb, S.F. and Archer, A.W., 2007. Soft-sediment deformation produced by tides in a meizoseismic area, Turnagain Arm, Alaska. Geology 35, 435-438.

Gupta, A. S., 1999. Controls on sedimentation in distal margin pallaeovalleys in the Early Tertiary Alpine foreland basin, southeastern France. Sedimentology, 46 (2), 357-384.

Hibert-Wolf, H.L., Simpson, E.L., Simpson, W.S., Tindall, S.E. and Wizevich, M.C., 2009. Insights into syndepositional fault movement in a foreland basin; trends in seismites of the Upper Cretaceous, Wahweap Formation, Kaiparowits Basin, Utah, USA. Basin Research, 21, 856-871.

Hohenegger, J., Ćorić, S. and Wagreich, M., 2014. Timing of the Middle Miocene Badenian Stage of the Central Paratethys. Geologica Carpathica, 65, 1, 55-66.

Holcová, K., Nehyba, S. and Scheiner, F., 2013. Taphonomical riddle in the epicontinental sea: variegated postmortal wanderings of foraminiferal tests in tectonically active basin (early Middle Miocene of the Central Paratethys). Abstracts of the TMS meeting 2013 Prague.

Jones, A.P. and Omoto, K., 2000. Towards establishing criteria for identifying trigger mechanisms for soft-sediment deformation: a case study of Late Pleistocene lacustrine sands and clays, Onikobe and Nakayamadaira Basins, northeastern Japan. Sedimentology, 47, 1211-1226.

Kováč M., 2000. Geodynamic, paleogeographical and structural development of the Miocene Carpatho-Pannonian region. New view on the Slovak Neogene basins. Veda, Bratislava, 76 pp.

Leichmann, J. and Hejl, E., 1996. Quaternary tectonics at the eastern border of the Bohemian Massif - New outcrop evidence. Geological Magazine, 1, 133, 103-105.

Lowe, D.R., 1975. Water escape structures in coarse-grained sediments. Sedimentology, 22, 157-204.

Lowe, D.R., 1976. Subaqueous liquefied and fluidized sediment flows and their deposits. Sedimentology, 23, 285-308.

Maltman, A., (Ed.) 1994. The Geological Deformation of Sediments. Chapman and Hall, London, 310 pp.

Maltman, A.J. and Bolton, A., 2003. How sediments become mobilized. Geological Society Special Publications, 216, 9-20.

Matsumoto, D., Naruse, H., Fujino, S., Surphawajruksakul, A., Jarupongsakul, T., Sakamura, N. and Murayama, M., 2008. Truncated flame structures within a deposit of the Indian Ocean Tsunami: evidence of syn-sedimentary deformation. Sedimentology, 55, 1559-1570.

Mazumder, R., Van Loon, A.J., Molina, J.M., Alfaro, P., Moretti, M. and Soria, J.M., 1998a. Soft-sediment deformation structures induced by cyclic stress of storm waves in tempestites (Miocene, Guadalquivir Basin, Spain). Terra Nova, 10, 145-150.

Mazumder, R., Van Loon, A.J. and Makoto, A., 1998b. Soft-sediment deformation structures in the Earth´s oldest seismites. Sedimentary Geology, 186, 19-26.

Mills, P.C., 1983. Genesis and diagnostic value of soft-sediment deformation structures – a review. Sedimentary Geology, 35, 83-104.

Molina, J.M., Alfaro, P., Moretti, M. and Soria, J.M., 1998. Soft-sediment deformation structures induced by cyclic stress of storm waves in tempestites (Miocene, Guadalquivir Basin, Spain). Terra Nova, 10, 145-150.

Montenat, C., Barrier, P., Ott d´Estevou, P. and Hibsch, C., 2007. Seismites: An attempt at critical analysis and classification. Sedimentary Geology, 196, 5-30.

Moretti, M., Alfaro, P., Caselles, O. and Canas, J.A., 1999. Modelling seismites with a digital shaking table. Tectonophysics, 304, 369-383.

Moretti, M. and Ronchi, A., 2011. Liquefaction features interpreted as seismites in the Pleistocene fluvio-lacustrine deposits of the Neuquén Basin (Northern Patagonia). Sedimentary Geology, 235, 200-209.

Nehyba, S., 1997. Miocene volcaniclastics of the CF in Czech Republic. Věstník Českého Geologického Ústavu, 72 (4), 311-327.

Nehyba, S. and Hladilová, Š., 2004. Relics of the most distal part of the Neogene foreland basin in SW Moravia. Bulletin of Geosciences, 79, 113-120.

Nehyba, S, Roetzel, R. and Maštera, L., 2012. Provenance analysis of the Permo-Carboniferous fluvial Sandstones of the southern part of the Boskovice Basin and the Zöbing Area (Czech Republic, Austria): Implications for paleogeographic reconstructions of the post-Variscan Collapse Basins. Geologica Carpathica, 62 (5), 365-382.

Nehyba, S. and Šikula, J., 2007. Depositional architecture, sequence stratigraphy and geodynamic development of the Carpathian Foredeep (Czech Republic). Geologica Carpathica, 58 (1), 53-69.

Nehyba, S., Tomanová-Petrová, P. and Zágoršek, K., 2008. Sedimentological and palaeoecological records of the evolution of the south western part of the Carpathian Foredeep (Czech Republic) during the early Badenian. Geological Quarterly, 52 (1), 45-60.

Nehyba, S., Tomanová-Petrová, P., Gilíková, H. and Horáková, M., 2009. Some remarks to the knowledge about depositional environment of Lower Badenian deposits at Oslavany. Geologické Výzkumy na Moravě a ve Slezsku, 16, 17-20. In Czech.

Nemec, W., 2005. Principles of lithostratigraphic logging and facies analyses. Institutt for geovitenskap, Univ. Bergen, 28 pp.

Nichols, R.J., Sparks, R.S.J. and Wilson, C.J.N., 1994. Experimental studies of the fluidization of layered sediments and the formation of fluid escape structures. Sedimentology, 41, 233-253.

Obermeier, S.F., 1998. Seismic liquefaction features: examples from paleoseismic investigations in the continental United States. Open-file Report 98–488. http://pubs.usgs.gov/of/of98-488.

Oliveira, C.M., Hodgson, D.M. and Flint, S.S., 2009. Aseismic controls on in situ soft-sediment deformation processes and products in submarine slope deposits of the Karoo Basin, South Africa. Sedimentology, 56, 1201-1225.

Owen, G., 1987. Deformation processes in unconsolidated sands. Geological Society Special Publications, 29, 11-24.

Owen, G., 1995. Soft-sediment deformation in Upper Proterozoic Torridonian sandstones (Applecross Formation) at Torridon, northwest Scotland. Journal of Sedimentary Research, A65, 495-504.

Owen, G., 1996a. Anatomy of a water-escape cusps in Upper Proterozoic Torridon Group sandstones, Scotland. Sedimentary Geology, 103, 117-128.

Owen, G., 1996b. Experimental soft-sediment deformation: structures formed by the liquefaction of unconsolidated sands and some ancient examples. Sedimentology, 43, 279-293.

Owen, G. and Moretti, M., 2011. Identifying triggers for liquefaction-induced soft-sediment deformation in sands. Sedimentary Geology, 235, 141-147.

Owen, G., Moretti, M. and Alfaro, P., 2011. Recognising triggers for soft-sediment deformation: Current understanding and future directions. Sedimentary Geology, 235, 133–140.

Papp, A., Cicha, I., Seneš, J. and Steininger, F.,1978. Badenian (Moravien, Wielicien, Kosovien). Chronostratigraphie und Neostratotypen, Miozän der Zentralen Paratethys, 6. VEDA, 594 pp. Bratislava.

Postma, G., 1983. Water escape structures in the context of a depositional model of a mass flow dominated conglomeratic fan-delta (Abrioja formation, Pliocene, Almeria Basin, Spain). Sedimentology, 30, 91-103.

Ross, J.A., Peakall, J. and Keevil, G.M., 2011. An integrated model of extrusive sand injectites in cohesionless sediments. Sedimentology, 58, 1693-1715.

Rossetti, D.F., 1999. Soft-sediment deformation structures in late Albian to Cenomanian deposits, Sao Luís Basin, northern Brazil: evidence for palaeoseismicity. Sedimentology, 46, 1065-1081.

Roštínský, P., Pospíšil, L. and Švábenský, O., 2013. Recent geodynamic and geomorphological analyses of the Diendorf–Čebín Tectonic Zone, Czech Republic. Tectonophysics, 599, 45-66.

Seilacher, A., 1984. Sedimentary structures tentatively attributed to seismic events. Marine Geology, 55, 1-12.

Scott, B. and Price, S., 1988. Earthquake-induced structures in young sediments. Tectonophysics, 147, 165-170.

Shiki, T., 1996. Reading of the trigger records of sedimentary events - a problem for future studies. Sedimentary Geology, 104, 249-255.

Sherman, D.J. and Greenwood, B., 1989. Hummocky cross-stratification and post-vortex ripples: length scales and hydraulic analysis. Sedimentology, 36 (6), 981-986.

Sims, J.D., 1975. Determining earthquake recurrence intervals from deformational structures in young lacustrine sediments. Tectonophysics, 29, 141-152.

Taşgin, C.K. and Türkmen, I., 2009. Analysis of soft-sediment deformation structures in Neogene fluvio-lacustrine deposits of Caybagi Firmation, Eastern Turkey. Sedimentary Geology, 218, 16-30.

Taşgin, C.K., Hűkmű, O., Türkmen, I. and Aksoy, E., 2011. Soft-sediment deformation structures in the late Miocene Şelmo Formation around Adıyaman area, Southeastern Turkey. Sedimentary Geology, 235: 277-291.

Van Loon, A.J., 2009. Soft-sediment synsedimentary deformations in siliciclastic sediments: an overview. Geologos, 15, 3-55.

Van Loon, A.J. and Wiggers, A.J., 1976. Metasedimentary „graben“ and associated structures in the lagoonal Almere Member (Groningen Formation, the Netherlands). Sedimentary Geology, 16, 237-254.

Wagreich, M., Pervesler, P., Khatun, M., Wimmer-Frey, I. and Scholger, R., 2008. Probing the underground at the Badenian type locality: geology and sedimentology of the Baden-Sooss section (Middle Miocene, Vienna Basin, Austria). Geologica Carpathica, 59, 375-394.

Walker, R.G. and James, N.P., 1992. Facies Models. Response to sea level changes. Geological Association of Canada, 380 pp., Toronto.

Wade, B.S., Pearson, P.N., Berggren, W.A. and Pälike, H., 2011. Review and revision of Cenozoic tropical planktonic foraminiferal biostratigraphy and calibration to the geomagnetic polarity and astronomical time scale. Earth-Science Reviews, 104, 111-142.

Wheeler, R.L., 2002. Distinguishing seismic from nonseismic soft-sediment structures:criteria from seismic-hazard analysis. GSA Special Paper, 359, 1-11.

Wysocka, A., Radwański, A. and Górka, M., 2012. Mykolaiv Sands in Opole Minor and beyond: sedimentary features and biotic content of Middle Miocene (Badenian) sand shoals of Western Ukraine. Geological Quarterly, 56 (3), 475-492.

Zágoršek, K., Holcová, K., Nehyba, S., Kroh, A. and Hladilová, Š., 2009. The invertebrate fauna of the Middle Miocene (Lower Badenian) sediments of Kralice nad Oslavou (Central Paratethys, Moravian part of the Carpathian Foredeep). Bulletin of Geosciences, 84 (3), 465-496.

Received: 5 February 2014
Accepted: 9 March 2014

Slavomír NEHYBA
Department of Geological Sciences, Faculty of Science, Masaryk University, Kotlářská 2, 611 37 Brno, Czech Republic;
slavek@sci.muni.cz